Current Chemistry Letters 13 (2024) 81–90

Contents lists available at GrowingScience

Current Chemistry Letters

homepage: www.GrowingScience.com

New biocidal hybrids bearing acridine and aminophosphonate Scaffolds against different bacterial pathogens

Heba Ramadan Gomaa[a], Abdel Aleem Hassan Abdel Aleem[a], Ayah Usama Salman[b] and Ibrahim E.T. El-Sayed[a*]

[a]*Department of Chemistry, Faculty of Science, Menoufia University, Shebin El-Koom, Menoufia, Egypt*
[b]*Department of Botany and Microbiology, Faculty of Science, Menoufia University, Shebin El-Kom 32511, Egypt*

C H R O N I C L E

Article history:
Received March 20, 2023
Received in revised form
June 9, 2023
Accepted August 17, 2023
Available online
August 17, 2023

Keywords:
Acridine
Lewis Acid
α-Aminophosphonate
Antibacterial

A B S T R A C T

New hybrids containing acridine and α-amino phosphonate scaffolds **6a-h** were synthesized by three one-pot reactions *via* Kabachnik–Fields reaction of 9-aminoacridine derivatives **3a-d**, aldehydes **4a,b** and triphenyl phosphite **5** in equimolar ratio under stirring at room temperature. The installation of the afforded hybrids was affirmed by different spectroscopic methods as IR, ^{1}HNMR, ^{13}CNMR, ^{31}P NMR, MS and elemental analysis. The antibacterial activities of hybrids **6a-h** were screened against both Gram-positive and Gram-negative bacteria of four pathogenic strains, comparable to ampicillin and chloramphenicol drugs. Most hybrids showed higher activity compared to the reference drugs. Notably, the antibacterial performance of **6c** was more substantial than other analogues with best minimum inhibitory concentration (MIC) and highest zone of inhibition (ZOI) of 31, 34, 35, 38 mm, against *Serratia marcescens*, *Streptococcus mutans, MRSA and Klebsiella pneumoniae* clinical isolates respectively. In addition, Transmission Electron Microscopes (TEM) was carried out to study the mode of action of **6c** with MRSA, the results confirmed that the titled hybrid caused the disruption of bacterial cell wall. Moreover, the time-dependent kill study revealed that the investigated compounds were time and dose-effective bactericidal agents and could be used as potential leads for further development and optimization of novel antibacterial agents.

1. Introduction

Antibiotic resistance is a global health concern that is expected to worsen in the near future. The misuse and overuse of antibiotics, as well as mutation owing to environmental changes and the gene transfer of bacteria, are the leading causes of antibiotic resistance.[1] From this perspective, searching for new efficient antibacterial agents to feed the preclinical pipeline is one of the challenges that researchers face in overcoming the emergence of antibiotic resistance to various bacterial strains. In this context, acridine along with its functional analogues are the most privileged pharmacophore in medicinal chemistry with diverse biological applications.[2-8] The pharmacological value of amino-acridines has been known for a long time and received much attention from many researchers due to their wide range of biological applications.[2] On the other hand, *α*-aminophosphonates are bioisosteres of naturally occuring amino acids with diverse pharmacological application.[9-24] The synthesis of aminoacridine derivatives and *α*-aminophosphonates has been introduced using a variety of synthetic processes.[9-11] A large number of analogues are displayed as antiviral, antifungal, antibacterial and antitumor agents.[2,9-11] However, there is still room for synthesizing new derivatives with potent antibacterial properties to increase medication availability and lessen the drug resistant bacteria issue. Encouraged by the aforementioned facts, it is anticipated that by combining two intrinsically biologically active scaffolds; such as amino acridine derivatives and aminophosphonates moieties, a synergistic effect would be anticipated for the resulting hybrid's structure when compared with each moiety

* Corresponding author.
E-mail address ibrahimtantawy@yahoo.co.uk Ibrahimtantawy2018@gmail.com (I. E.T. El-Sayed)

doi: 10.5267/j.ccl.2023.8.007

independently. In this study, certain novel acridine-aminophosphonate hybrids with or without carbon spacer will be synthesized and evaluated for their antibacterial action against both Gram-negative and Gram-positive bacteria aiming to reach the best substitution and activity for the synthesized hybrids, **Fig. 1**.

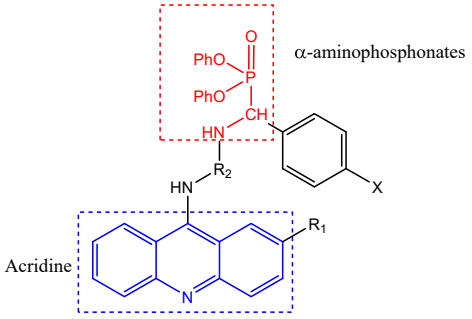

Fig. 1. Design of aminoacridine- α-aminophosphonate hybrids

2. Results and Discussion

2.1 Chemistry

The preparation of 9-aminoacridine derivatives **3a-d** was achieved as reported before[24] by nucleophilic substitution reaction of 9-chloroacridine **1a, b** with hydrazine **2a** or ethane-1, 2-diamine **2b** under reflux to afford the 9-aminoacridine derivatives **3a-d** in good yields as depicted in **Scheme 1.**

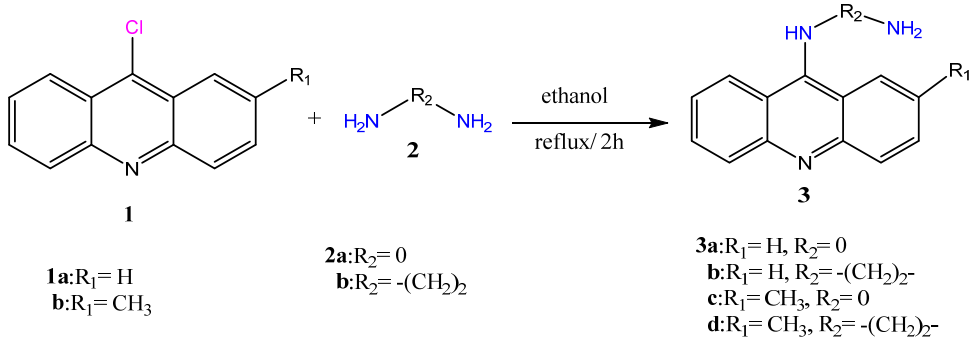

1

1a:R_1= H
b:R_1= CH_3

2

2a:R_2= 0
b:R_2= -$(CH_2)_2$

3

3a:R_1= H, R_2= 0
b:R_1= H, R_2= -$(CH_2)_2$-
c:R_1= CH_3, R_2= 0
d:R_1= CH_3, R_2= -$(CH_2)_2$-

Scheme 1. Synthesis of 9-aminoacridine derivatives 3a-d

The synthesis of α-aminophosphonate derivatives bearing acridine core structure **6a-h** was achieved in good yields via Kabachink-field reaction by three one-pot reaction of equimolar ratio of 9-aminoacridine derivatives **3a-d**, aldehydes **4a,b**, triphenyl phosphite **5** in acetonitrile with presence of 10% mole of lithium perchlorate (LiClO4) as a Lewis acid catalyst. as illustrated in **Scheme 2.**

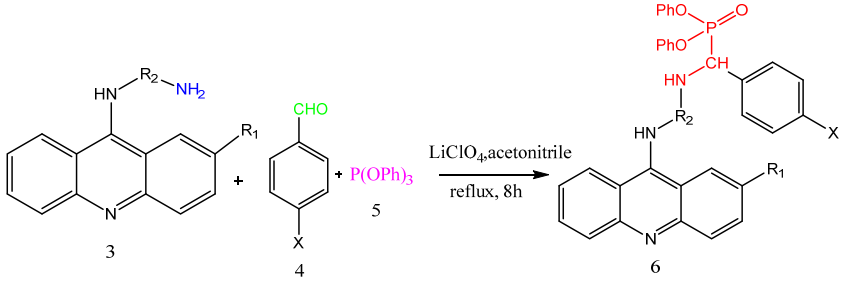

3

3a:R_1= H, R_2= 0
b:R_1= H, R_2= -$(CH_2)_2$-
c:R_1= CH_3, R_2= 0
d:R_1= CH_3, R_2= -$(CH_2)_2$-

4

4a:X= H
b:X= CH_3

5

6

6a:R_1= H, R_2= 0, X= H
b:R_1= H, R_2= 0, X= $N(CH_3)_2$
c:R_1= H, R_2= -$(CH_2)_2$-, X= H
d:R_1= H, R_2= -$(CH_2)_2$-, X= $N(CH_3)_2$
e:R_1= CH_3, R_2= 0, X= H
f:R_1= CH_3, R_2= 0, X= $N(CH_3)_2$
g:R_1= CH_3, R_2= -$(CH_2)_2$-, X= H
h:R_1= CH_3, R_2= -$(CH_2)_2$-, X=$N(CH_3)_2$

Scheme 2. Synthesis of α-aminophsophonate bearing acridine core

The chemical structures of the synthesized hybrids **6a-h** were fully elucidated through FT-IR spectroscopy, NMR (^{1}H-, & ^{13}C-) techniques, MS spectrometry, and elementary analysis (CHN). The results in good agreement with the proposed chemical structures, and the known compounds showed data consistent with the literature data. Referring to the FT-IR spectra of **6a-h**, the absorption bands ranged from ν^- = 3253 to 3279 cm^{-1}, indicated secondary amine (>NH), aromatic (C-H) ranged from 3028 to 3198 cm^{-1}. Whereas the bands of aliphatic (C-H), and (-P=O), were recorded at ν^- = 2882 to 2988, and 1209 to 1327 cm^{-1}, respectively. Moreover, ^{13}C-NMR spectra of hybrids **6a-h** gave representative peaks of (P-C-H) chiral carbon displayed at δ = 46,54 to 58,40 ppm in addition to the other expected carbon signals for aliphatic and aromatic carbons. The phosphorus atoms were individually resonated as a single peak at δ = 14.08 and 14.85 ppm, respectively. Furthermore, the mass spectra of the target hybrids are in conformity with the assigned structure and showed molecular ion peaks corresponding to their molecular formula (for details cf. the supporting information). Additionally, the elemental analysis of the as-prepared manifested the successful reaction with the expected products. Accordingly, the proposed mechanistic route of the reaction occurred through two major steps: a) the *in-situ* generation of Schiff base via activation of the formyl group by Lewis acid (LA) catalyst; this facilitated the condensation reaction between aminoacridine derivatives **3** and aldehydes via nucleophilic addition of nitrogen lone pair to the electrophilic carbon of the activated carbonyl group of (-CHO). b) the nucleophilic attack of the (triphenyl phosphite) phosphorus atom to the electrophilic carbon of the imine moiety (>C=N-), followed by the extrusion of phenol molecule through formation of the *in-situ* phosphonium salt and hydroxy phosphite intermediates **Scheme 3**.

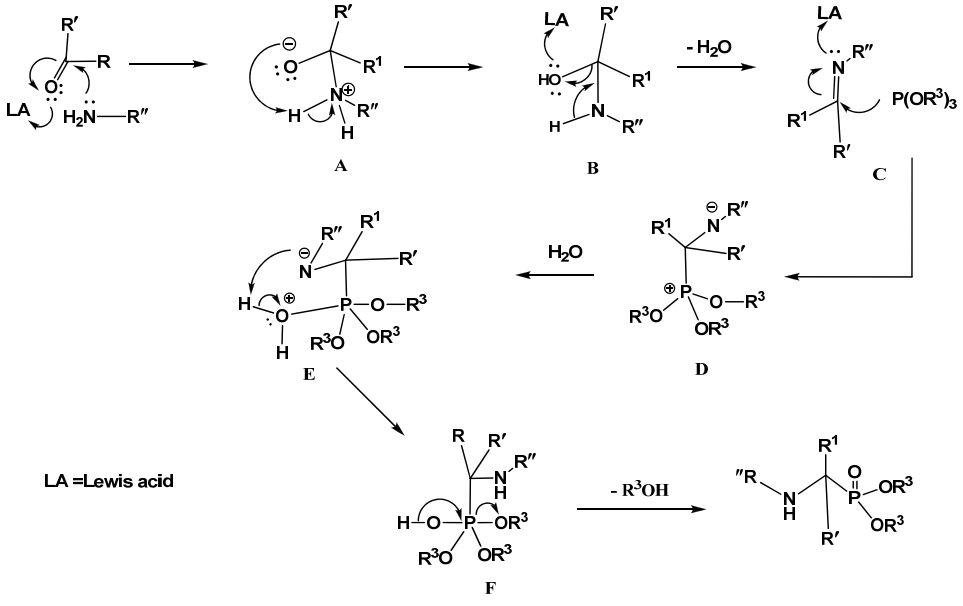

Scheme 3. Proposed mechanism for hybrids formation

2.2 In vitro antibacterial screening

The *In vitro* screening of the synthesized hybrids **6a-h** was done with concentration 40 mg/mL against clinical isolates Gram positive bacteria such as MRSA and *Streptococcus mutans* and Gram-negative bacteria such as *Serratia marcescens* and *Klebsiella pneumonia*.[25-29] The following results presented the potency of these hybrids **6a-h** against these clinical isolates compared to the control drug ampicillin and chloramphenicol with concentration 80 mg/mL.

2.2.1 Antibacterial screening of acridine – α-aminophosphonate hybrids against MRSA

The screening results of synthesized hybrids **6a-h** against *MRSA* showed the antibacterial activity of all hybrids except **6f** which has zone of inhibition lower than the the standard drugs ampicillin and chloramphenicol. Notably, hybrid **6c** displayed the best activity with zone of inhibition of 35 mm and minimum inhibitory concentration (MIC) of 0.078 mg /mL compared to the reference drugs as shown in **Table 1.**

Table 1. The antibacterial screening of synthesized hybrids against *MRSA* clinical isolates

Compounds	ZOI	*MRSA*			*MRSA ATCC 43300*		
		MBC	MIC	MBC/MIC	MBC	MIC	MBC/MIC
6a	19 ±1.00	1.25	0.312	4 (+)	2.5	0.625	4(+)
6b	17±0.60	0.625	0.312	2(+)	1.25	0.625	2(+)
6c	35±1.00	0.156	0.078	2(+)	0.312	0.156	2(+)
6d	18±0.60	1.25	0.625	2(+)	2.5	1.25	2 (+)
6e	23±0.60	0.078	0.039	2(+)	0.312	0.078	4 (+)
6f	13±1.00	1.25	0.625	2(+)	2.5	1.25	2 (+)
6g	33±0.60	0.156	0.039	4 (+)	0.312	0.078	4(+)
6h	31±0.60	0.156	0.039	4 (+)	0.312	0.078	4 (+)
Ampicillin	14.77±0.60	6.25	3.13	2(+)	6.25	1.56	4 (+)
Chloramphenicol	14.32±0.60	3.13	0.78	4(+)	12.5	8	1.6(+)

2.2.2 Antibacterial screening of acridine – α-aminophosphonate hybrids against Streptococcus mutans

The antibacterial potency of hybrids **6a-h** was further evaluated against *Streptococcus mutans* clinical isolates, and the results was depicted in **Table 2.** Notably, all hybrids have revealed higher activity, especially **6c** displayed a significant activity among other with zone of inhibition of 34 mm at a minimum inhibitory concentration (MIC) of 0.078 mg/mL compared to the reference drugs.

Table 2. The antibacterial screening of synthesized hybrids against *Streptococcus mutans* clinical isolates

Compounds	ZOI	*Streptococcus mutans*			*Streptococcus mutans ATCC 35668*		
		MBC	MIC	MBC/MIC	MBC	MIC	MBC/MIC
6a	19±1.00	1.25	0.312	4 (+)	2.5	0.625	4(+)
6b	17±0.60	1.25	0.625	2(+)	2.5	1.25	2(+)
6c	34±1.00	0.156	0.078	2(+)	0.312	0.156	2(+)
6d	18±0.60	0.625	0.312	2(+)	2.5	0.625	4 (+)
6e	28±0.60	0.078	0.039	2(+)	0.156	0.078	2 (+)
6f	15±1.00	1.25	0.625	2(+)	2.5	1.25	2 (+)
6g	22±0.60	0.625	0.312	4 (+)	1.25	0.625	2(+)
6h	28±0.60	0.078	0.039	2 (+)	0.312	0.078	4 (+)
Ampicillin	12±1	3.13	1.565	2 (+)	6.25	3.13	2(+)
Chloramphenicol	12.7±0.6	6.25	1.56	4 (+)	12.5	6.25	2(+)

*2.2.3 Antibacterial screening of acridine – α-aminophosphonates hybrids **6a-h** against Klebsiella pneumonia*

As reported in **Table 3**, all hybrids of **6a-h** were screened against *Klebsiella pneumonia*. Compound **6c** showed the highest zone of inhibition of (38 mm) at a minimum inhibitory concentration (MIC) of 0.078 mg /mL compared to the reference drugs. While other hybrids showed variable activity ranging from 17 to 28 mm and the least effective ones were **6d** and **6f**.

Table 3. The antibacterial screening of synthesized hybrids against *Klebsiella pneumoniae* clinical isolates

Compounds	ZOI	*Klebsiella pneumonia*			*Klebsiella pneumoniae ATCC 700603*		
		MBC	MIC	MBC/MIC	MBC	MIC	MBC/MIC
6a	19±1.00	0.625	0.156	4 (+)	1.25	0.312	4(+)
6b	18±0.60	0.625	0.312	2(+)	1.25	0.625	2(+)
6c	38±1.00	0.078	0.019	4 (+)	0.156	0.039	4(+)
6d	17±0.60	0.625	0.312	2(+)	2.5	0.625	4 (+)
6e	18±0.60	0.312	0.156	2(+)	0.625	0.312	2 (+)
6f	17±1.00	1.25	0.625	2(+)	2.5	1.25	2 (+)
6g	22±0.60	0.156	0.078	2(+)	0.312	0.156	2(+)
6h	28±0.60	0.312	0.078	4 (+)	0.312	0.156	2 (+)
Ampicillin	14.3±0.6	8	4	2(+)	6.25	3.125	2(+)
Chloramphenicol	8.7±0.6	3.13	1.565	2 (+)	6.25	1.56	4 (+)

2.2.4 Antibacterial screening of acridine – α-aminophosphonate hybrids against Serratia marcescens

Results listed in **Table 4** showed that all hybrids **6a-h** at low dose is more effective than the positive reference standard. Hybride **6c** showed the highest zone of inhibition of 31 mm with minimum inhibitory concentration (MIC) of 0.078 mg /mL compared to the reference drugs.

Table 4. The antibacterial screening of acridine – α-aminophosphonate against *Serratia marcescens* clinical isolates

Compounds	ZOI	*Serratia marcescens*			*Serratia marcescens ATCC13880*		
		MBC	MIC	MBC/MIC	MBC	MIC	MBC/MIC
6a	17±1.00	0.312	0.078	4 (+)	0.625	0.156	4(+)
6b	22±0.60	0.625	0.312	2(+)	1.25	0.625	2(+)
6c	31±1.00	0.156	0.078	2(+)	0.312	0.156	2(+)
6d	19±0.60	1.25	0.625	2(+)	2.5	1.25	2 (+)
6e	18±0.60	0.625	0.312	2(+)	1.25	0.625	2 (+)
6f	17±1.00	1.25	0.625	2(+)	2.5	1.25	2 (+)
6g	29±0.60	0.156	0.039	4 (+)	0.312	0.078	4(+)
6h	23±0.60	0.312	0.078	4 (+)	0.312	0.156	2 (+)
Ampicillin	12±1	3.13	1.565	2 (+)	6.25	3.13	2(+)
Chloramphenicol	12.7±0.6	6.25	1.56	4 (+)	12.5	6.25	2(+)

From the above-mentioned results, it is notable that synthesized 9-amioacridine- α-aminophosphonate hybrids showed remarkable activity against Gram positive and Gram negative clinical isolate bacteria, especially **6c** containing 9-aminoethylamino acridine with potent activity against these clinical isolates.

2.2.5 Time-kill assay:

Time kill assay was performed to assess bacteriostatic or bactericidal nature and relationship between the concentration of the *test* compound and the net growth . The broth macro-dilution method to determine the minimum inhibitory concentration (MIC) and minimum bactericidal concentration (MBC) values were executed according to the CLSI guidelines. The test compounds were serially twofold diluted in DMSO to achieve the range of test concentrations of 6.250–0.039 mg/mL and then placed into each well of a 96-well microplate. An inoculum suspension with density of 105 CFU/ml exponentially growing bacterial cells was added into each well. The 96-well microplates were incubated at 37°C for 24 h. As depicted in **Table 5**, all hybrids **6a-h** had a MBC/MIC ratio ≤ 4, (bactericidal) with dose dependent, as illustrated in Table 5, and Fig. 2.

Table 5. MIC minimum inhibitory concentration (mg/mL), MBC minimum bactericidal concentration (mg/mL), MBC/MIC ratio for bacteriostatic or bactericidal activity for the synthesized hybrids **6a-h.**

Compounds	MBC	MIC	MBC/MIC
6a	1.25	0.312	4 (+)
6b	0.625	0.312	2(+)
6c	0.156	0.078	2(+)
6d	1.25	0.625	2(+)
6e	0.078	0.039	2(+)
6f	1.25	0.625	2(+)
6g	0.156	0.039	4 (+)
6h	0.156	0.039	4 (+)
Ampicillin	6.25	3.13	2(+)
Chloramphenicol	3.13	0.78	4(+)

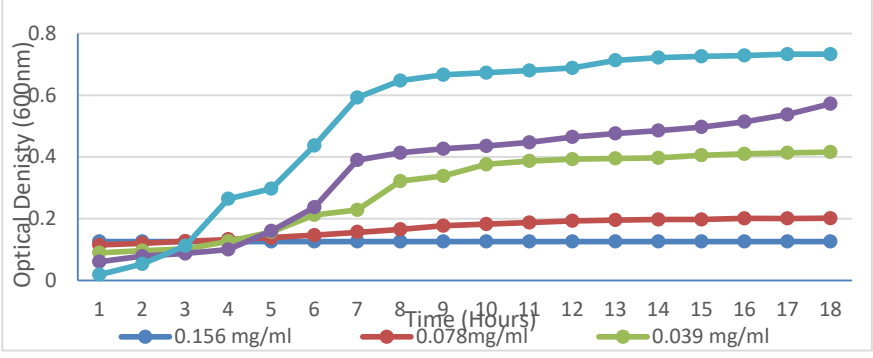

Fig. 2. Time-kill assay for synthesized hybrids **6a-h**

2.2.6 Transmission Electron Microscopes (TEM) Assay

The structural appearance of untreated MRSA as depicted in Fig. 3 with treated **6c** as shown in **Fig. 4**, was analyzed using TEM. The figures of treated MRSA showed an altered MRSA cell membrane and dead bacterial cells after exposure to hybrid **6c**. The figures also show vacuoles created in the cytoplasm. These micrographs demonstrate that **6c** disrupt the

MRSA bacterial cell wall, resulting in cell death; these effects were amplified and can be described as bactericidal. The figure also depicts increased cell death because of fewer cells, which is consistent with the observations made with untreated MRSA in **Fig. 3.**

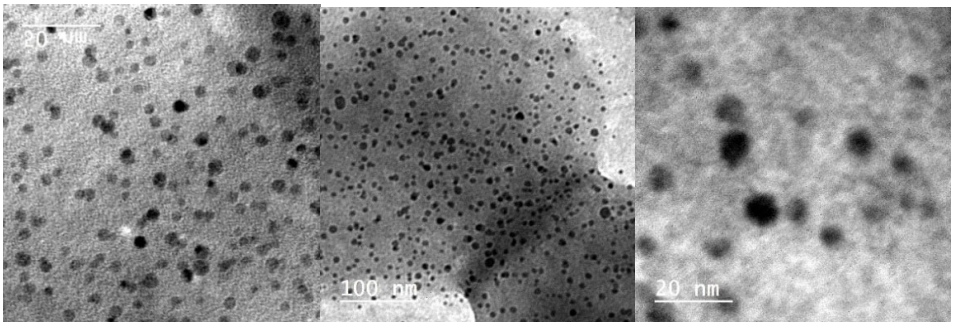

Fig. 3. TEM micrographs of untreated methicillin-resistant *Staphylococcus aureus* (MRSA)

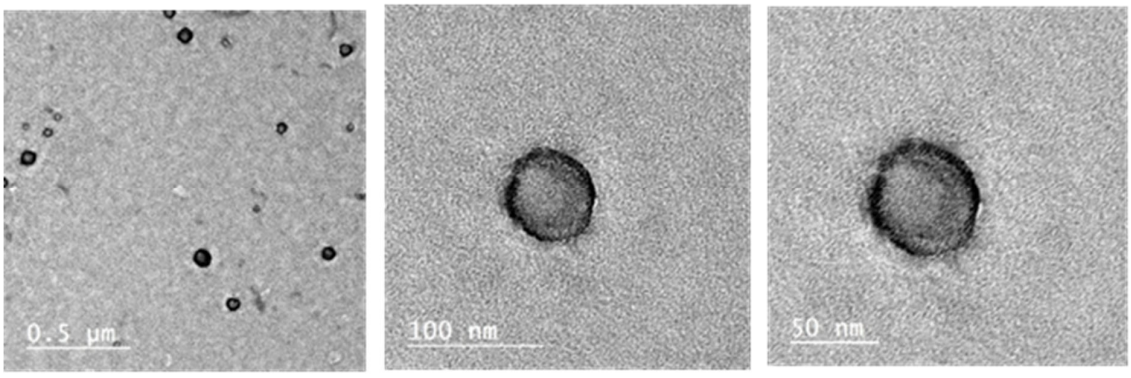

Fig. 4. TEM micrographs of methicillin-resistant *Staphylococcus aureus* (MRSA) treated with **6c** showing incomplete cell wall destruction, cell death

3. Conclusions

New hybrids **6a-h** bearing acridine and aminophosphonate scaffolds were prepared in good yields. The structures of the hybrids were established based on spectroscopic data. The antibacterial activity for all synthesized hybrids was evaluated and displayed activity higher than the first line antibiotics ampicillin and chloramphenicol used in this study. In addition, the TEM study of **6c** proved its mechanism of action where a damage in both cell wall and membrane was observed with the appearance of damaged vacuoles in cell cytoplasm. Thus, the time-dependent kill study revealed that the investigated compounds were time and dose-effective bactericidal agents. This study presents a preliminary step forward towards synthesis and development of new lead hybrids with potential antibacterial performances in the medical field.

4. Experimental

4.1. Materials and Methods

^{1}H NMR,^{13}C NMR and ^{31}P NMR experiments were carried out with the Bruker magnet system 400’54 Ascend/R (USA) 400, 100 and 161 MHz for ^{1}H NMR, ^{13}C NMR, and ^{31}P NMR respectively. FTIR spectroscopy, were performed with Alpha-Bruker ATR mode (USA) at Zagazig University. Elemental analysis (C,H,N) was performed at the Microanalytical unit at Cairo University on CHNS-932 (LECO) Vario Elemental Analyzers. Mass spectroscopy was performed on Direct Inlet part to mass analyzer in GCMS model with ISQ single quadrupole thermos-scientific Electron Impact mode (UK) at the Regional Center for Mycology and Biotechnology, Al-Azhar University. Melting points (m.p.) were determined using the Stuart scientific melting point apparatus and are uncorrected. The in vitro antibacterial screening was executed at the Department of Botany and Microbiology, Faculty of Science, Menoufia University. All reactions were monitored by using thin layer chromatography (TLC) on Kiesel gel F254 pre-coated plates (Merck). All reagents and solvents were purchased from commercial sources and used without further purification. The synthesized 9-chloroacridine **1** and 9-aminoacridine derivatives **3a-d** were prepared in good yields as reported in literature.[24]

4.2. General procedure for synthesis of aminoacridine- α-aminophosphonate hybrids:

To aminoacridine derivatives **3** (1mmol), aryl aldehydes **4** (1mmol), triphenyl phosphite **5** (1mmol) in acetonitrile (3 mL), 20 mol% of lithium perchlorate ($LiClO_4$) was added under magnetic stirring. Further, the reaction mixture was stirred

under ambient conditions and the reaction was monitored via qualitative thin layer chromatography (TLC) using hexane-methylene chloride (3:1) as eluent mixture till the complete consumption of the starting materials after 8 hrs. Eventually, the solvent was removed and the precipitated products were filtered off under vacuum, washed with methanol, dried to afford the hybrids **6a-h** in good yields.

Diphenyl((2-(acridin-9-yl)hydrazinyl)(phenyl)methyl) phosphonate (**6a**):
Dark brown solid, yield (0.150 g, 60%) m.p >300 ºC; FT IR (KBr) ν cm^{-1}: 3273 (NH), 3095 (CHAr), 2945 (CH), 1633(C=C_{Ar}), 1595(C=N), 1288(P=O), 1156(C-C). ^{1}H-NMR δ: 6.27 (m, 1H, CH-P), 7.19–8.32 (m, 23H, CH_{Ar}), 11.84 (br.s, 2H, 2NH). ^{13}C- NMR δ: 48.63, 120.54, 121.11, 123.24, 124.22, 124.89, 125.95, 127.55, 128.55, 129.18, 129.75, 130.11, 130.53, 132.30, 138.60,143.54, 149.91, 154.56, 166.86. ^{31}P-NMR δ: 1.64 ppm. Elemental analysis calc. (%) for ($C_{32}H_{26}N_3O_3P$): C, 72.31; H, 4.93; N, 7.91. Found: C, 71.18; H, 4.12; N, 7.03. MS, m/z ($C_{32}H_{26}N_3O_3P$) calcd, 531.17 ; found, 531.31 [M^+].

Diphenyl((2-(acridin-9-yl)hydrazinyl)(4-(dimethylamino)phenyl) methyl)phosphonate (**6b**):
Brownish red solid, yield (0.244 g, 75%) m.p >300 ºC, FT IR (KBr) ν cm^{-1}: 3272(NH) , 3028 (CHAr),2988(CH), 1633(C=C_{Ar}), 1593(C=N), 1287(P=O), 1204(C-C). ^{1}H-NMR δ: 2.99(m, 6H, 2CH_3), 6.74(m, 1H, CH-P), 7.11–8.81 (m, 22H, CH_{Ar}), 10.52 (br.s,2H, 2NH). ^{13}C- NMR δ: 41.30,58.40, 117.88,120.87, 120.92, 120.94, 121.42, 122.55, 126.45, 129.53, 129.81, 133.87, 141.43, 153.66, 177.24. ^{31}P-NMR δ : 0.15 ppm. Elemental analysis calc. (%) for ($C_{34}H_{31}N_4O_3P$): C, 71.07; H, 5.44; N, 9.75.. Found: C, 69.87; H, 4.99; N, 9.13. EI MS, m/z ($C_{34}H_{31}N_4O_3P$) calcd, 574.21 ; found, 574.86 [M^+].

Diphenyl(((2-(acridin-9-ylamino)ethyl)amino)(phenyl)methyl) phosphonate (**6c**):
Yellow solid, yield (0 .124 g, 73%) m.p 278-280 ºC , FT IR (KBr) ν cm^{-1}: 3269 (NH), 3072 (CHAr) ,2882(CH), 1637(C=C_{Ar}), 1587(C=N), 1209(P=O), 1147(C-C). ^{1}H NMR δ: 4.43 (br.s , 4H, 2CH_2), 6.31 (m, 1H, CH-P), 7.19–8.33 (m, 23H, CH_{Ar}), 11.84 (s, 2H, 2NH). ^{13}C- NMR δ: 56.03 ,117.37 ,120.48 ,120.97,125.99,133.41,140.93,176.78. ^{31}P-NMR δ: -0.33 ppm. Elemental analysis calc. (%) for ($C_{34}H_{30}N_3O_3P$): C, 72.98; H, 5.40; N, 7.51. Found: C, 71.88; H, 5.14; N, 6.88. EI MS, m/z ($C_{34}H_{30}N_3O_3P$) calcd, 559.20 ; found, 559.68 [M^+].

Diphenyl (((2-(acridin-9-ylamino) ethyl)amino)(4-(dimethylamino) phenyl)methyl)phosphonate (**6d**).
Dark yellow solid, yield (0.286 g, 72%), m.p 290-292 ºC, FT IR (KBr) ν cm^{-1}: 3272(NH), 3029 (CHAr), 2972(CH),1633(C=C_{Ar}), 1594(C=N), 1261(P=O), 1205(C-C). ^{1}H-NMR δ: 3.03(s,6H,2 CH_3) , 4.63(br.s 4H, 2CH2), 6.74 (m, 1H, CH-P), 6.76–8.23 (m, 21H, CH_{Ar}), 9.65 (br.s, 1H, NH), 11.95 (br.s, 1H, NH). ^{13}C- NMR δ: 41.33, 56.60, 111.04, 112.36, 114.72, 115.05, 115.24, 117.37, 118.78, 120.49, 120.98, 126.01, 129.36, 129.54, 133.42, 140.92,143.25, 143.88, 165.29, 173.22,176.79. ^{31}P-NMR δ: -0.26 ppm. Elemental analysis calc. (%) for ($C_{36}H_{35}N_4O_3P$): C, 71.75; H, 5.85; N, 9.30. Found: C, 70.78; H, 5.13; N, 8.87. EI MS, m/z ($C_{36}H_{35}N_4O_3P$) calcd, 602.24 ; found, 602.13 [M^+].

Diphenyl((2-(2-methylacridin-9-yl)hydrazineyl)(phenyl)methyl) phosphonate (**6e**):
Black solid, yield (0.230 g, 69.5%) m.p 263-265 ºC, FT IR (KBr) ν cm^{-1}: 3274 (NH) ,3064(CH_{Ar}), 2922 (CH), 1616(C=C_{Ar}), 1580(C=N), 1252(P=O), 1208(C-C). ^{1}H-NMR δ: 2.37 (s, 3H, CH_3), 6.73 (m, 1H, CH-P), 7.13–8.32 (m, 22H, CH_{Ar}), 10.57 (s, 1H, NH). ^{13}C- NMR δ: 47.54, 115.08, 120.12, 120.53, 123.12, 124.62, 127.71, 129.13, 129.37, 129.59, 129.82, 130.03, 130.80, 131.33, 131.88, 136.52, 136.69, 138.50, 140.64, 143.24, 143.89,165.29. ^{31}P-NMR δ : - 0.15 ppm. Elemental analysis calc. (%) for ($C_{32}H_{28}N_3O_3P$): C, 72.65; H, 5.17; N, 7.70. Found: C, 71.46; H, 4.94; N, 6.93. EI-MS, m/z ($C_{32}H_{28}N_3O_3P$) calcd, 545.19 ; found, 545.34 [M^+].

Diphenyl((4-(dimethylamino)phenyl)(2-(2-methylacridin-9-yl) hydrazineyl)methyl)phosphonate (**6f**):
Dark violet solid, yield (0.200g, 78%) m.p > 300 ºC, FT IR (KBr) ν cm^{-1}: 3278 (NH), 3198 (CHAr) ,2955(CH) , 1616(C=CAr), 1581(C=N), 1253(P=O), 1210(C-C). ^{1}H-NMR δ: 2.28(s,3H, CH_3), 3.65 (s, 6H,2 CH_3), 5.92 (S, 1H, CH-P), 7.08–8.89 (m, 21H, CH_{Ar}), 9.66(br.s, 1H, NH), 10.56(br.s,1H,NH). ^{13}C- NMR δ: 41.26, 56.81, 115.86, 116.67, 119.50, 125.16, 125.42, 130.32, 131.11, 131.49, 131.93, 132.14, 138.92, 143.53, 145,24. ^{31}P-NMR δ : 1.35 ppm. Elemental analysis calc. (%) for ($C_{37}H_{37}N_4O_3P$): C, 71.42; H, 5.65; N, 9.52. Found: C, 70.13; H, 5.21; N, 8.87. EI MS, m/z ($C_{37}H_{37}N_4O_3P$) calcd, 588.23 ; found, 588.65 [M^+].

Diphenyl(((2-((2-methylacridin-9-yl)amino)ethyl)amino)(phenyl) methyl)phosphonate **(6g):**
Yellow solid, yield (0 .150 g, 62%) m.p 268-270 ºC, FT IR (KBr) ν cm^{-1}: 3253 (NH), 3039 (CHAr), 2939 (CH), 1631(C=C_{Ar}), 1587(C=N), 1245(P=O), 1214(C-C). ^{1}H NMR δ: 2.22 (s, 3H, CH_3), 2.39 (m,2H, CH_2), 4.42 (br.s , 2H, CH_2), 6.21 (m, 1H, CH-P), 7.13–8.14 (m, 22H, CH_{Ar}), 10.02 (s, 1H, NH), 11.69 (br.s, 1H, NH). ^{13}C- NMR δ:50.45, 120.36, 120.70, 121.29, 122.39, 125.22, 125.98, 128.93, 129.24,129.35, 130.06, 130.27, 132.11, 132.21, 132.63, 133.20, 134.37,134.90, 138.99, 142.03, 154.73, 157.32, 167.53.^{31}P-NMR δ: -2.50 ppm. Elemental analysis calc. (%) for ($C_{35}H_{32}N_3O_3P$): C, 73.28; H, 5.62; N, 7.33. Found: C, 72.19; H, 5.21; N, 6.78. EI MS, m/z ($C_{35}H_{32}N_3O_3P$) calcd, 573.22 ; found, 573.66 [M^+].

Diphenyl ((4-(dimethylamino)phenyl)((2-((2-methylacridin-9-yl) amino) ethyl)amino)methyl)- phosphonate **(6h):**
Yellow solid, yield (0.236 g, 71%) m.p 215-217 ºC, FT IR (KBr) ν cm^{-1}: 3279 (NH), 3172 (CH_{Ar}),2982(CH), 1631(C=C_{Ar}), 1575(C=N), 1327(P=O), 1218(C-C). ^{1}H-NMR δ: 2.21 (s, 3H, CH_3), 3.03(s,6H,2 CH_3), 4.50 (s,2H,CH_2), 6.74 (m, 1H, CH-P), 7.13–8.19 (m, 21H, CH_{Ar}), 9.66 (s, 2H, 2NH). ^{13}C- NMR δ: 41.35, 50.07, 111.05, 113.45, 115.20, 118.76, 120.49, 122.40, 122.62, 125.51, 129.34, 132.74, 133.37, 135.44, 156.12, 157.30. ^{31}P-NMR δ: -1.99 ppm. Elemental analysis: calc. (%) for ($C_{37}H_{37}N_4O_3P$): C, 72.06; H, 6.05; N, 9.09. Found: C, 70.87; H, 5.67; N, 8.42. EI MS, m/z ($C_{37}H_{37}N_4O_3P$) calcd, 616.26; found, 616.12 [M^+]

References

1 Murray C.J., Ikuta K.S., Sharara F., Swetschinski L., Aguilar G.R., Gray A., Han C., Bisignano C., Rao P., and Wool E.J.T.L. **(2022)** Global burden of bacterial antimicrobial resistance in 2019: a systematic analysis. 399, 629-655.

2 Baliwada A., Rajagopal K., Varakumar P., Raman K., and Byran G. **(2022)** A Review on Acridines as Antiproliferative Agents. *Mini Rev Med Chem*, 22 (21) 2769-2798.

3 Kožurková M., Sabolová D., and Kristian P. **(2017)** a review on acridinylthioureas and its derivatives: biological and cytotoxic activity. *Journal of Applied Toxicology*, 37 (10) 1132-1139.

4 Sadowski M., Utnicka J., Wójtowicz A., and Kula K. **(2023)** The global and local Reactivity of C, N-diarylnitryle imines in [3+2] cycloaddition processes with trans-β-nitrostyrene according to Molecular Electron Density Theory: A computational study. *Current Chemistry Letters*, 12, 421–430.

5 Kula K., and Zawadzińskaa K. **(2021)** Local nucleophile-electrophile interactions in [3+2] cycloaddition reactions between benzonitrile N-oxide and selected conjugated nitroalkenes in the light of MEDT computational study. *Current Chemistry Letters,* 10, 9–16.

6 Zawadzinska K., Ríos-Gutiérrez M., Kula K., Wolinski P., Mirosław B., Krawczyk T., and Jasinski R. **(2021)** The Participation of 3,3,3-Trichloro-1-nitroprop-1-ene in the [3+2] Cycloaddition Reaction with Selected Nitrile N-Oxides in the Light of the Experimental and MEDT Quantum Chemical Study. *Molecules*, 26 (22) 6774.

7 Kula K., Łapczuk A., Sadowski M., Kras J., Zawadzinska K., Demchuk O. M., Gaurav G.K, Wróblewska A., and Jasiński R. **(2022)** On the Question of the Formation of Nitro-Functionalized 2,4-Pyrazole Analogs on the Basis of Nitrylimine Molecular Systems and 3,3,3-Trichloro-1-Nitroprop-1-Ene. *Molecules*, 27 (23) 8409.

8 Kula K. and Sadowski M. **(2023)** Regio- and stereoselectivity of [3+2] cycloaddition reactions between (Z)-1-(anthracen-9-yl)-N-methyl nitrone and analogs of trans-β-nitrostyrene on the basis of MEDT computational study. *Chem. Heterocycl. Compd*., 59 (3) 138-144.

9 El-Tantawy A. I., Elmongy E. I., Elsaeed S. M., Abdel Aleem A. A. H., Binsuwaidan R., Eisa W. H., Salman A. U., Elharony N. E., and Attia N. F. **(2023)** Synthesis, Characterization, and Docking Study of Novel Thioureidophosphonate-Incorporated Silver Nanocomposites as Potent Antibacterial Agents*. Pharmaceutics,* 15 (6) 1666.

10 Elsherbiny D. A., Abdelgawad A. M., El-Naggar M. E., El-Sherbiny R. A., El-Rafie M. H., and El-Sayed I. E. T. **(2020)** Synthesis, antimicrobial activity, and sustainable release of novel α-aminophosphonate derivatives loaded carrageenan cryogel. *International Journal of Biological Macromolecules*, 163, 96-107.

11 Boshta N. M., Elgamal E. A., and El-Sayed I. E. T. **(2018)** Bioactive amide and α-aminophosphonate inhibitors for methicillin-resistant Staphylococcus aureus (MRSA). *Monatshefte für Chemie - Chemical Monthly,* 149, 2349-2358.

12 Ravi N., Venkatanarayana M., Sharathbabu H., and Babu K. R.. **(2021)** Synthesis of novel α-aminophosphonates by methanesulfonic acid catalyzed Kabachnik–Fields reaction. *Phosphorus, Sulfur, and Silicon and the Related Elements*, 196 (11) 1018-1024.

13 Hamed M., El Gokha A., El-Tantawy A. I., and Sabry, M. **(2015)** Synthesis and Antimicrobial Activity of Novel α-Aminophosphonates Bearing Pyrazoloquinoxaline Moiety*. International Journal of Pharmaceutical Sciences Review and Research*, 34 (33) 205-213.

14 Danne A., Akolkar S., Deshmukh T., Siddiqui M., and Shingate B. **(2019**) One-pot facile synthesis of novel 1,2,3-triazole-appended α-aminophosphonates. *Journal of the Iranian Chemical Society,* 16, 953-961.

15 Sreelakshmi P, Maheshwara R. N., Santhisudha S., Mohan G., and Saichaithanya N. **(2019)** Nano Sb_2O_3 catalyzed green synthesis, cytotoxic activity, and molecular docking study of novel α-aminophosphonates. *Medicinal Chemistry Research,* 28, 528-544.

16 El Boraey H. A. L., El Gokha A. A., and El-Sayed I. E. T. **(2015)** Transition metal complexes of α-aminophosphonates Part I: synthesis, spectroscopic characterization, and in vitro anticancer activity of copper(II) complexes of α-aminophosphonates. *Medicinal Chemistry Research,* 24, 2142-2153.

17 El Gokha A. A., Ahmed A. A. S., Abdelwahed N. A. M., and El Sayed I. E. T. **(2016)** Synthesis and Antimicrobial Activity of Novel mono- and bis-α-Aminophosphonate Derivatives. *International Journal of Pharmaceutical Sciences Review and Research,* 36 (2) 35-39.

18 El Gokha A. A., Ghanim I. M. S., Abdel Megeed A. El. S., El-khabiry S., and El-Sayed I. E. T. **(2016)** Synthesis and antibacterial activity of novel α-aminophosphonates bearing a quinoline moiety. *IJSPR*, 7, 181-189.

19 Xu Y., Yan K., Song B., Xu G., and Yang S. **(2006)** Synthesis and Antiviral Bioactivities of α-Aminophosphonates Containing Alkoxyethyl Moieties. *Molecules*, 11 (6), 666-676.

20 Pietrusiewicz K. M., Szwaczko K., Mirosław B., Dybała I., Jasinski R., and Demchuk O. M. **(2019)** New Rigid Polycyclic Bis(phosphane) for Asymmetric Catalysis. *Molecules*, 24, 571.
21 Demchuk O. M., Jasinski R., Strzelecka D., Dziuba K., Kula K., Chrzanowski J., and Krasowska D. **(2018)** A clean and simple method for deprotection of phosphines from borane complexes. *Pure and Applied Chemistry*, 90 (1) 49–62.
22 Jasiński R., Demchuk O. M., and Babyuk D. **(2017)** A Quantum-Chemical DFT Approach to Elucidation of the Chirality Transfer Mechanism of the Enantioselective Suzuki–Miyaura Cross-Coupling Reaction. *Journal of Chemistry*, 3617527.
23 Demchuk O. M., and Jasiński R. **(2016)** Organophosphorus ligands: Recent developments in design, synthesis, and application in environmentally benign catalysis. *Phosphorus Sulfur and Silicon and the Related Elements*, 191, 245-253.
24 Ahmed A. A., Awad H. M., El-Sayed I. E. T., and El Gokha A. A. **(2020)** Synthesis and antiproliferative activity of new hybrids bearing neocryptolepine, acridine and α-aminophosphonate scaffolds. *J Iran Chem Soc,* 17, 1211–1221.
25 Ozturk S., and Ercisli S. **(2006)** Chemical composition and in vitro antibacterial activity of Seseli libanotis. *World J. Microbiol. Biotechnol*, 22, 261–265.
26 Daoud A., Malika D., Bakari S., Hfaiedh N., Mnafgui K., Kadri A., and Gharsallah N. **(2015)** Assessment of polyphenol composition, antioxidant and antimicrobial properties of various extracts of Date Palm Pollen (DPP) from two Tunisian cultivars. *Arab. J. Chem*., 12, 3075–3086.
27 Eloff J. **(1998)** A Sensitive and Quick Microplate Method to Determine the Minimal Inhibitory Concentration of Plant Extracts for Bacteria. *Planta Med*. 64, 711–713.
28 Petersen P., Wang T., Dushin R., Bradford P. A. **(2004)** Comparative In Vitro Activities of AC98-6446, a Novel Semisynthetic Glycopeptide Derivative of the Natural Product Mannopeptimycin α, and Other Antimicrobial Agents against Gram-Positive Clinical Isolates. *Agents Chemother*., 48, 739–746.
29 Datta A., Ghoshdastidar S., and Singh M. **(2011)** Antimicrobial Property of Piper betel Leaf against Clinical Isolates of Bacteria. *Int. J. Pharm. Sci.*, 2, 104–109.